Applied Surface Science 457 (2018) 93–97

Contents lists available at ScienceDirect

Applied Surface Science

journal homepage: www.elsevier.com/locate/apsusc

Full Length Article

Structural and chemical characterization of CdSe-ZnS core-shell quantum dots

N. Fernández-Delgado[a,*], M. Herrera[a], A.H. Tavabi[b], M. Luysberg[b], R.E. Dunin-Borkowski[b], P.J. Rodriguez-Cantó[c], R. Abargues[c,d], J.P. Martínez-Pastor[d], S.I. Molina[a]

[a] Department of Material Science, Metallurgical Engineering and Inorganic Chemistry, IMEYMAT, University of Cádiz, Puerto Real 11510, Cádiz, Spain
[b] Ernst Ruska-Centre for Microscopy and Spectroscopy with Electrons and Peter Grünberg Institute, Forschungszentrum Jülich, 52425 Jülich, Germany
[c] INTENANOMAT S.L., Paterna 46980, Spain
[d] Institute of Material Science, University of Valencia, Valencia 46071, Spain

ARTICLE INFO

Keywords:
Semiconductors
Quantum dots
Core-shell nanoparticles
HRTEM
HAADF-STEM
EDX

ABSTRACT

The structural and compositional properties of CdSe-ZnS core-shell quantum dots (QDs) with a sub-nm shell thickness are analyzed at the atomic scale using electron microscopy. QDs with both wurtzite and zinc blende crystal structures, as well as intermixing of the two structures and stacking faults, are observed. High-angle annular dark-field scanning transmission electron microscopy suggests the presence of a lower atomic number epitaxial shell of irregular thickness around a CdSe core. The presence of a shell is confirmed using energy dispersive X-ray spectroscopy. Despite the thickness irregularities, the optical properties of the particles, such as photoluminescence and quantum yield, show clear enhancement after growth of the ZnS shell.

1. Introduction

Colloidal QDs[1] are of increasing interest for applications in photovoltaics [1,2], lighting [3] and sensing [4], as a result of their extraordinary properties, such as their tunable band gaps, as well as the reduced cost of their fabrication. For numerous applications, such QDs need to have small diameters, often between 2.5 and 5 nm [5]. The quality of the QD surfaces also influences their performance [4,5]. In particular, surface defects that include dangling bonds can create non-radiative sites that deteriorate optical properties such as QY[2] [6]. In order to overcome the detrimental effects of such defects, the encapsulation of QDs by shells has attracted attention, as it has been found to improve their performance with respect to bare colloidal QDs [2,4]. The formation of a shell has additional advantages, such as preventing the release of the non-environmentally-friendly heavy metals and providing stability against photo-oxidation. If the band gap of the shell is larger than that of the core, then the system is known as type I and electrons and holes are confined in the core. This is the case for CdSe-ZnS core-shell QDs, for which the shell has been reported to increase the QY and PL[3] intensity with respect to CdSe QDs [8]. As a result, CdSe-ZnS colloidal QDs are used extensively in the photovoltaic field [7,8]. During the synthesis of such QDs, parameters such as size, shape and high mono-dispersion must be controlled, as they have a strong influence on optical properties. For example, critical values of CdSe core size can lead to the escape of electrons from the core to the shell [9]. The core size can be controlled by the temperature and concentration of the precursors [10], which should be optimized. The structural properties of the shell, such as its thickness and crystallinity, also have a crucial impact on the optoelectronic properties of core-shell QDs [11]. It is therefore possible to obtain tunable emission from CdSe-ZnS QDs by controlling their shell thickness [8]. Vinayakan et al. reported an optimum ZnS shell thickness of 1.3–2.2 MLs[4], in order to avoid the formation of misfit dislocations [12]. Despite the importance of shell thickness, its influence is often only studied using indirect techniques such as PL and QY [11,10]. In order to achieve further progress, direct structural and compositional information about the core, the shell and the relationship between them are essential.

TEM[5] can be used to obtain direct local information about the

* Corresponding author.
E-mail address: natalia.fernandezdelgado@uca.es (N. Fernández-Delgado).
[1] quantum dots
[2] quantum yield
[3] photoluminescence
[4] monolayers
[5] transmission electron microscopy

https://doi.org/10.1016/j.apsusc.2018.06.149
Received 16 April 2018; Received in revised form 28 May 2018; Accepted 16 June 2018
Available online 28 June 2018

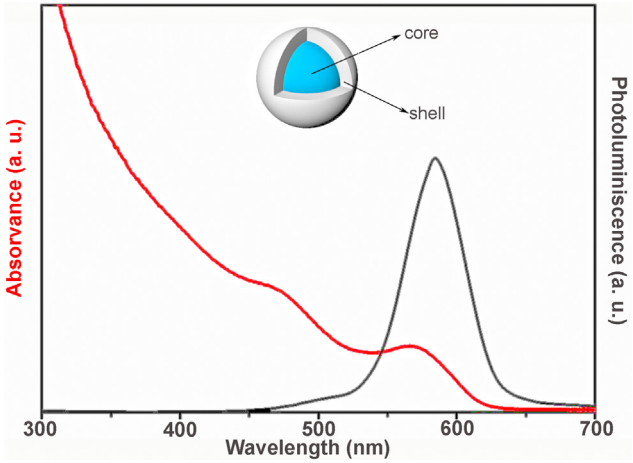

Fig. 1. Absorbance and PL spectra of CdSe-ZnS core-shell QDs in solution.

structural properties of materials. HRTEM[6] can be used to obtain atomic scale information about the crystalline quality of colloidal core-shell QDs, such as CdS-ZnS [12,13] or CdSe-ZnS-CdS [14] QDs. Interfaces in core-shell Pd-Pt nanoparticles [15] and anisotropic cation exchange evolution at interfaces in PbSe-CdS core-shell nanorods have been studied successfully using HAADF-STEM[7] [16]. The latter technique has proved to be useful for the study of Au QDs with Pd shells as thin as 2 nm [17]. Here, we use (S)TEM to study the structural properties of CdSe-ZnS colloidal core-shell QDs with sub-nm shell thicknesses. We find that the QDs adopt a mixture of zinc blende and wurtzite crystal structures and have dimensions that are consistent with optical measurements. The presence of an epitaxial shell of irregular thickness is identified using atomically resolved HAADF STEM and EDX[8].

2. Materials and methods

2.1. CdSe core synthesis

Highly luminescent CdSe QDs were prepared by a conventional synthesis route based on a hot injection method [18]. Briefly, a mixture of CdO (5 mmol) and oleic acid (30 mmol) in ODE[9] was heated in vacuum at 120 °C for 30 min to remove any residual moisture. The mixture was heated to 250 °C to ensure complete solution of the precursors under N_2. A transparent solution of Se (3.2 mmol) and TOP[10] (16 mmol) was injected swiftly at 250 °C and left to react for 5 min. The QDs were then purified by several successive precipitation and redispersion steps with a mixture of acetone and methanol and redispersed in octadecene for further processing.

2.2. CdSe-ZnS core-shell synthesis

Core-shell synthesis was carried out following the SILAR method, which is based on alternating injections of Zn and S precursors into a solution containing CdSe nanocrystals, in order to synthesize CdSe-ZnS core-shell nanocrystals. The Zn precursor solution (0.1 M) was prepared by dissolving ZnO (0.13 mmol) in oleic acid (0.9 mmol) and ODE (1 mL) at 310 °C. The S precursor (0.1 M) was prepared by dissolving sulfur (0.13 mmol) in ODE (1.34 mL) at 180 °C. Once clear solutions were obtained, the Cd and S solutions were allowed to cool to 120 °C and room temperature, respectively.

The amount of Zn and S precursor required for each layer was determined by the number of surface atoms of a given size for the core-shell nanocrystal. The average thickness of one monolayer of ZnS was taken to be 0.31 nm. One additional monolayer of growth therefore increases the shell thickness by up to 0.62 nm [5]. The typical synthesis of core-shell CdSe-ZnS nanocrystals consisted of mixing CdSe crystals (2.7 nm in diameter, 3.75×10^{-4} mmol) with 25 mL of ODE in a three-neck flask. The flask was pumped down at 100 °C for 30 min to remove any residual moisture. The reaction mixture was further heated to 240 °C under Ar for the injections. The first injection comprised 0.53 mL of the Zn precursor solution at 0.1 mL/min. After 30 min, 0.53 mL of the S precursor solution was injected slowly at 0.1 mL/min. After 30 min, the second monolayer of the shell was formed by adding 0.68 mL of the Zn precursor solution and, after 30 min, the same amount of the S solution was injected at the same rate. The reaction was cooled to room temperature and the product was purified by two successive precipitations and redispersion cycles using methanol and chloroform. Finally, the QDs were dispersed in chloroform at a concentration of 20 mg/mL.

2.3. Characterization

Optical absorbance spectra were recorded at room temperature using an ultraviolet-visible Perkin-Elmer Lambda 20 spectrophotometer. PL spectra were measured at room temperature upon excitation of the samples with a CW GaN laser (404 nm) or DSPP diode laser (533 nm). In both cases, the excitation power was fixed to be approximately 15 kW cm^2. The QY for CdSe QDs was determined using an integrated sphere (Hamamatsu model C9920-0). CdSe-ZnS specimens for the (S)TEM study were prepared by dropping the solution containing the QDs onto holey C grids. Then, a H_2/Ar plasma treatment was used for 50 s to clean the samples, in particular from residual organic compounds from the colloidal synthesis process. An FEI Titan Themis Cubed TEM and an FEI Titan G2 80-200 ChemiSTEM equipped with a Super-X EDX system were used for (S)TEM measurements. The accelerating voltages used were 200 kV for imaging and 80 kV for EDX.

3. Results and discussion

Fig. 1 shows absorbance and PL spectra recorded from CdSe-ZnS core-shell QDs in solution. The first excitonic absorption is located at 570 nm, while a second exciton is located close to 460 nm. The emission band is centered at 590 nm with a FWHM[11] of 60 nm. The QY improves from 15% to 50% after the formation of a ZnS shell of thickness 0.62 nm. The QY enhancement is attributed to the shell passivation of non-radiative surface trap sites, such as dangling bonds [7]. The measured optoelectronic properties suggest that the CdSe QDs are fully covered by a ZnS shell, which leads to an enhancement of PL and QY.

Fig. 2(a) shows an HRTEM image, in which where several CdSe-ZnS QDs are visible. One of the QDs has been marked by a circle. As expected, the QDs are crystalline. Their average diameter is measured to be 3.8 ± 0.2 nm, which is consistent with the nominal values (2.70 nm core and 0.62 nm shell). Fig. 2(b) shows a histogram of the measured QD size distribution. Most of the QDs have diameters of between 3.5 and 4.5 nm. Their sizes and optical properties are consistent with each other, according to empirical functions reported by Lu et al., which correlate size with excitonic peak position [19].

The crystal structures of the QDs were determined from the high-resolution micrographs. Fig. 2(c) and (d) show HRTEM images of two QDs and their Fourier transforms. Fig. 2(c) reveals the typical zigzag pattern of the wurtzite crystal structure viewed along [0 1 0], with a measured lattice spacing of 0.36 nm, in agreement with the expected crystalline structure. A different crystal structure is found in the QD

[6] high resolution TEM
[7] high angle annular dark field-scanning TEM
[8] energy dispersive X-ray
[9] octadecene
[10] trioctylphosphine
[11] Full Width at Half Maximum

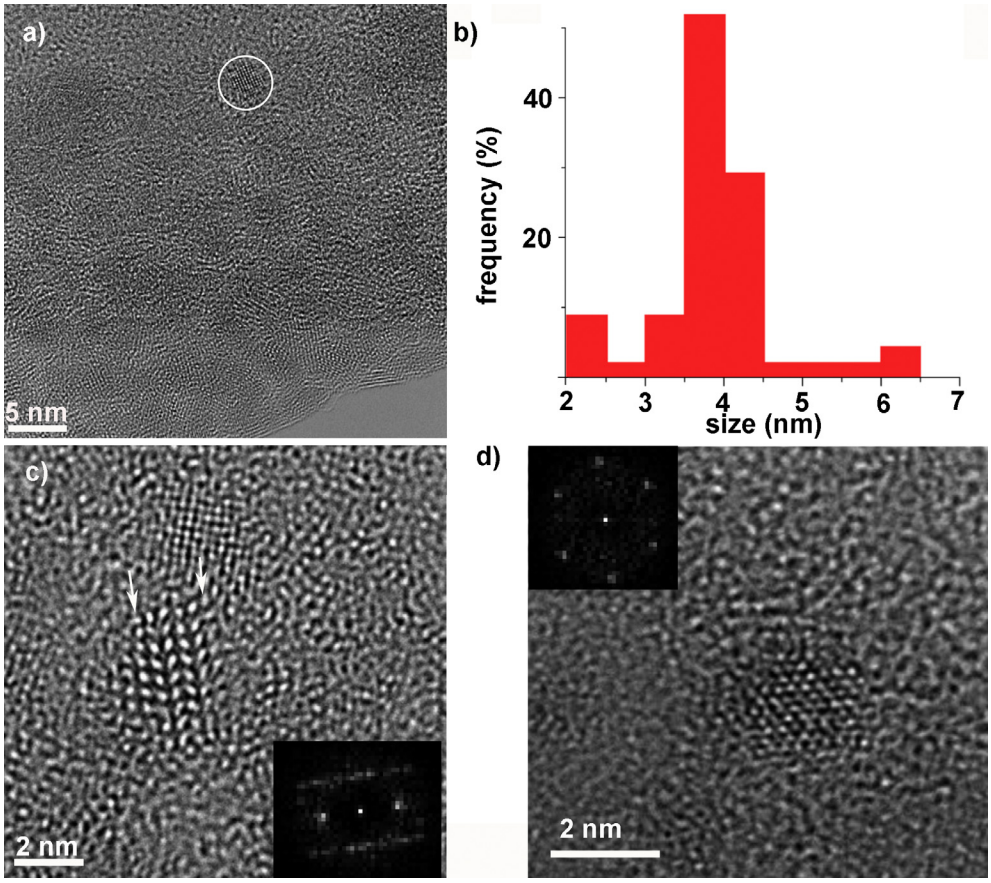

Fig. 2. (a) HRTEM image of CdSe-ZnS core-shell QDs supported on a holey C grid; (b) Histogram of the size distribution of the CdSe-ZnS QDs analyzed; (c and d) QDs with (c) wurtzite and (d) zinc blende structures, with Fourier transforms included as insets.

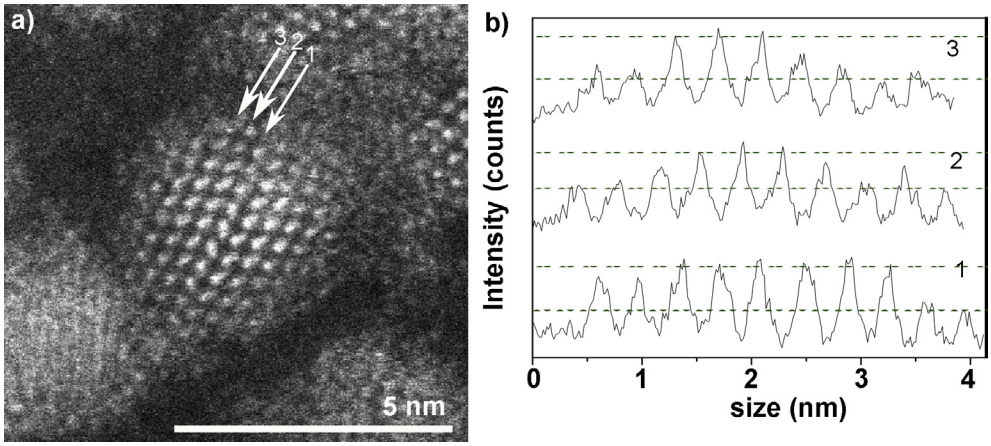

Fig. 3. (a) HAADF STEM image of CdSe-ZnS core-shell QDs; (b) Intensity profiles obtained from the atomic columns marked with arrows in (a), with dotted lines included to guide the eye.

shown in Fig. 2(d). According to the Fourier transform and the measured lattice spacing of 0.21 nm, the particle is a CdSe-ZnS core-shell QD with a zinc blende crystal structure, viewed along the [1 1 1] zone axis. In general, the sample contains QDs with both zinc blende and wurtzite structures. Stacking faults are also observed in both structures. For example, in Fig. 2(c) the wurtzite (ABAB) symmetry is interrupted by stacking faults (ABCABC). Polymorphism in CdSe nanocrystals (zinc blende and wurtzite) is common [16,17] because the structures have similar internal energies and small structural differences [21], leading to frequent stacking faults in such QDs [22]. Xia et al. suggested [22] that the zinc blende structure in CdSe-ZnS QDs results in better optoelectronic properties, because their QY improves in comparison to the wurtzite structure.

With regard to the shell, a different crystalline structure at the edge of the QDs was not observed in the HRTEM images, suggesting that it may have formed epitaxially. This is a general requirement for core-shell QDs with satisfactory optoelectronic properties, as the quality of the interface has an important effect on QY [22]. Epitaxial growth is favored when the lattice mismatch between the shell and the core is low, as in CdSe-CdS (4% lattice mismatch) [23]. In our material, CdSe-ZnS has an 11% lattice mismatch. However, PL [24] and QY [13] measurements suggest that the shell grows epitaxially. As the HRTEM

images cannot directly confirm the presence of the shell in the CdSe-ZnS QDs, results obtained using alternative techniques are reported below.

HAADF STEM is a well-established technique to distinguish the core from the shell in the present CdSe-ZnS QDs, as the intensity is related to the average atomic number Z in the material. Thus, elements with higher Z should result in higher values of intensity. The average value of Z for the CdSe core (Z_{Cd} = 48 and Z_{Se} = 34) is almost double than that of the ZnS shell (Z_{Zn} = 30 and Z_S = 16). Therefore, the two materials are expected to be distinguishable in HAADF STEM images. Fig. 3(a) shows an HAADF STEM image of a CdSe-ZnS QD with the wurtzite structure. The atomic columns that are located at the centers of the QDs have higher intensities than those at their edges. However, interpretation of the observed HAADF STEM intensity variations is not straightforward, as the specimen thickness also plays an important role in determining the intensity distribution. In spherical CdSe-ZnS QDs, the edges of the particles are expected to show reduced intensity in HAADF STEM images because of the smaller value of Z for ZnS compared to CdSe, but also because the thickness of the material in this region is lower. Image simulations of spherical particles have shown that the intensity decrease due to the spherical shape is gradual [25], whereas that due to a change in the average value of Z is sharper [26]. Fig. 3(b) shows intensity profiles obtained from the positions marked with arrows in Fig. 3 a). Dotted lines have been included as a guide for the eye. A clear reduction in HAADF STEM intensity is observed at the edge of the particle (on both sides in profiles 3 and 4 and on the right side in profile 5). The atomic columns in the center of the particle have similar intensity values, as do the columns at the edge of the QD. However, there is not a clear reduction in intensity, suggesting the presence of a non-uniform lower Z shell around a CdSe core. Similar results were obtained for other QDs. The reduction in intensity at the edges of core-shell QDs has previously been used to detect shells in QDs [14,20]. However, such intensity variations are more clear for QDs that have larger diameters and thicker shells. In the present case, the detection of a shell with a thickness of 2 ML is very challenging. Moreover, because the shell thickness may be irregular [13], the interpretation of the projected intensity is complicated. Therefore, additional techniques are required, in order to establish the formation and distribution of the ZnS shell.

The CdSe-ZnS core-shell QDs were analyzed further using EDX. Fig. 4(a) shows an EDX map, in which several QDs can be identified. The interpretation of information about the shell thickness from such EDX maps is challenging, as elements that are in the shell are also expected to be present all around the particle in three dimensions. In addition, because of the sizes of the QDs, the amount of material available to obtain EDX data in STEM mode is limited. The small size of each QD also makes it sensitive to electron beam irradiation, requiring the use of short exposure times and leading to a reduced number of EDX counts during analysis. As a result, conventional composition quantification methods cannot be used to obtain information about the elemental distribution. We therefore used a methodology based on the evaluation of projected net count ratios of different elements along EDX linescans. For example, an EDX linescan was taken from the QD marked *A* along the marked line (linescan 1). The net counts in the linescan corresponding to each element were summed, and a ratio between the net counts of elements from the shell and from the core was calculated, with a focus on Zn in the shell and Cd in the core. The Zn/Cd ratio is expected to be higher at the edge of the QD, where the element from the core (Cd) is reduced. In contrast, in the central part of the QD the Zn/Cd ratio should be lower because the amount of Cd is expected to be greater. This procedure was carried out for parallel linescans across the QD. The resulting Zn/Cd ratios are shown in the form of a graph in Fig. 4(b). The analysis reveals a higher Zn/Cd ratio at the edges of the particle, and a reduced ratio in the center of the QD. The results therefore suggest the presence of a shell around the CdSe core. However, in other CdSe-ZnS core-shell QDs different results were sometimes obtained. Fig. 4(c) shows the Zn/Cd ratio for the QD marked *B* in Fig. 4(a). An increase in Zn/Cd ratio compared to the center of the particle is observed on the left edge of the QD, whereas such an increase is not found on the right side, suggesting that the shell is not uniform around the particle and that thickness variations occurred during its formation. Such thickness variations are expected to have a direct influence on the functional properties of the QDs, such as photostability [27] and emission brightness because of their effect on the absorption cross-section [11]. Irregularities of the shell could also lead to non-optimal passivation of the surface of the core and to degradation of the optoelectronic properties. It may be possible to improve homogenization of the shell by annealing, as shown from PL results for CdSe-CdS (with 3 ML shells) [28].

4. Conclusions

The synthesis of CdSe-ZnS QDs using hot injection and the SILAR method have been shown to produce epitaxial shells in particles with both zinc blende and wurtzite crystal structures. The presence of the shell has been confirmed using HAADF STEM and EDX measurements, although shell thickness irregularities were observed. The optical properties of these CdSe-ZnS QDs, such as PL and QY, are enhanced when a ZnS shell is grown on the CdSe.

Acknowledgments

This work was supported by the Spanish MINECO (projects TEC2014-53727-C2-1-R, -2-R and TEC2017-86102-C2-2-R) and Junta de Andalucía (PAI research group TEP-946). The research leading to these results has received co-funding from the European Union.

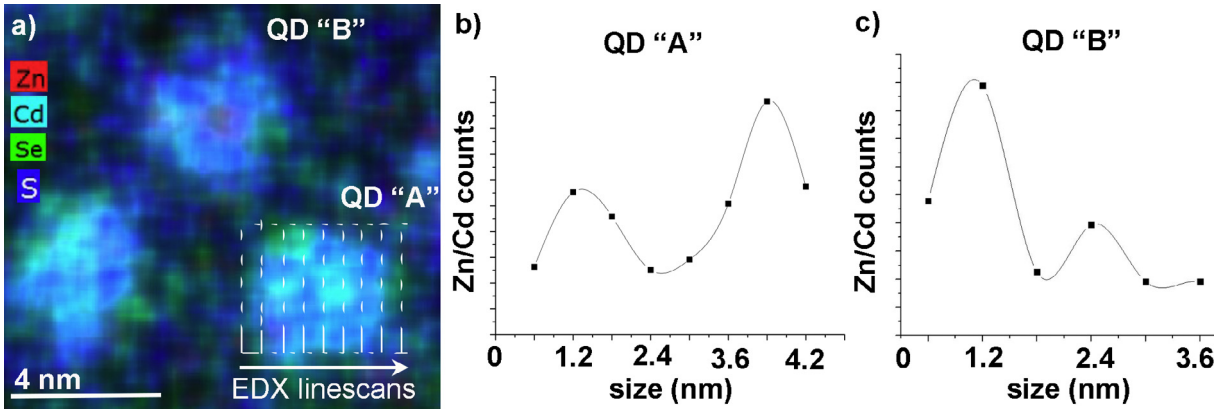

Fig. 4. (a) EDX map of CdSe-ZnS core-shell QDs, with two CdSe-ZnS core-shell QDs marked A and B; (b and c) Zn/Cd net count ratios for (b) QD A and (c) QD B.

References

[1] J. Jean, T.S. Mahony, D. Bozyigit, M. Sponseller, J. Holovský, M.G. Bawendi, V. Bulović, Radiative efficiency limit with band tailing exceeds 30% for quantum dot solar cells, ACS Energy Lett. 2 (2017) 2616–2624.

[2] S. Jindal, S.M. Giripunje, S.B. Kondawar, P. Koinkar, Green synthesis of $CuInS_2$/ZnS core-shell quantum dots by facile solvothermal route with enhanced optical properties, J. Phys. Chem. Solids 114 (2018) 163–172.

[3] Y. Shirasaki, G.J. Supran, M.G. Bawendi, V. Bulović, Emergence of colloidal quantum-dot light-emitting technologies Yasuhiro, Nat. Photo. 7 (2013) 933.

[4] T.H. Kim, C.S. Lee, S. Kim, J. Hur, S. Lee, K.W. Shin, Y.Z. Yoon, M.K. Choi, J. Yang, D.H. Kim, T. Hyeon, S. Park, S. Hwang, Fully stretchable optoelectronic sensors based on colloidal quantum dots for sensing photoplethysmographic signals, ACS Nano 11 (2017) 5992–6003.

[5] P. Reiss, M. Protière, L. Li, Core/shell semiconductor nanocrystals, Small 5 (2009) 154–168.

[6] X. Liu, Y. Zhang, T. Yu, X. Qiao, R. Gresback, X. Pi, D. Yang, Optimum quantum yield of the light emission from 2 to 10 nm hydrosilylated silicon quantum dots, Part. Part. Syst. Charact. 33 (2016) 44–52.

[7] D. Vasudevan, R.R. Gaddam, A. Trinchi, I. Cole, Core-shell quantum dots: properties and applications, J. Alloys Compd. 636 (2015) 395–404.

[8] A. Gadalla, M.S. Abd El-Sadek, R. Hamood, Characterization of CdSe core and CdSe/ZnS core/shell quantum dots synthesized using a modified method, Chalcogenide Lett. 14 (2017) 239–249.

[9] A. Zouitine, A. Ibral, E. Assaid, F. Dujardin, E. Feddi, Spatial separation effect on the energies of uncorrelated and correlated electron-hole pair in CdSe/ZnS and InAs/InP core/shell spherical quantum dots, Superlatt. Microstruct. 109 (2017) 123–133.

[10] J.S. Owen, E.M. Chan, H. Liu, A.P. Alivisatos, Precursor conversion kinetics and the nucleation of cadmium selenide nanocrystals, J. Am. Chem. Soc. 132 (2010) 18206–18213.

[11] M. Chern, T.T.H. Nguyen, A.H. Mahler, A. Dennis, Shell thickness effects on quantum dot brightness and energy transfer, Nanoscale 9 (2017) 16446–16458.

[12] R. Vinayakan, T. Shanmugapriya, P.V. Nair, P. Ramamurthy, K.G. Thomas, An approach for optimizing the shell thickness of core-shell quantum dots using photoinduced charge transfer, J. Phys. Chem. C 111 (2007) 10146–10149.

[13] Z. Yu, L. Quo, H. Du, T. Krauss, J. Silcox, Shell distribution on colloidal CdSe/ZnS quantum dots, Nano Lett. 5 (2005) 565–570.

[14] H.S. Pisheh, N. Gheshlaghi, H. Ünlü, The effects of strain and spacer layer in CdSe/CdS/ZnS and CdSe/ZnS/CdS core/shell quantum dots, Phys. E Low-Dimen. Syst. Nanostruct. 85 (2017) 334–339.

[15] W. Gao, Z.D. Hood, M. Chi, Interfaces in heterogeneous catalysts: advancing mechanistic understanding through atomic-scale measurements, Acc. Chem. Res. 50 (2017) 787–795.

[16] M. Casavola, M.A. Van Huis, S. Bals, K. Lambert, Z. Hens, D. Vanmaekelbergh, Anisotropic cation exchange in PbSe/CdSe core/shell nanocrystals of different geometry, Chem. Mater. 24 (2012) 294–302.

[17] E.A. Larios-Rodríguez, F.F. Castillón-Barraza, R. Herrera-Urbina, U. Santiago, A. Posada-Amarillas, Synthesis of aucorepdshell nanoparticles by a green chemistry method and characterization by HAADF-STEM imaging, J. Clust. Sci. 28 (2017) 2075–2086.

[18] P.J. Rodriguez-Canto, R. Abargues, H. Gordillo, I. Suarez, V. Chirvony, S. Albert, J. Martinez-Pastor, UV-patternable nanocomposite containing CdSe and PbS quantum dots as miniaturized luminescent chemo-sensors, RSC Adv. 5 (2015) 19874–19883.

[19] W.W. Yu, L. Qu, W. Guo, X. Peng, Experimental determination of the extinction coefficient of CdTe, CdSe, and CdS nanocrystals, Chem. Mater. 15 (2003) 2854–2860.

[20] F.A. La Porta, J. Andrés, M.S. Li, J.R. Sambrano, J.A. Varela, E. Longo, Zinc blende versus wurtzite ZnS nanoparticles: control of the phase and optical properties by tetrabutylammonium hydroxide, Phys. Chem. Chem. Phys. 16 (2014) 20127–20137.

[21] C.Y. Yeh, Z.W. Lu, S. Froyen, A. Zunger, Zinc-blendewurtzite polytypism in semiconductors, Phys. Rev. B 46 (1992) 10086–10097.

[22] X. Xia, Z. Liu, G. Du, Y. Li, M. Ma, Wurtzite and zinc-blende CdSe based core/shell semiconductor nanocrystals: Structure, morphology and photoluminescence, J. Lumin. 130 (2010) 1285–1291.

[23] X. Peng, M.C. Schlamp, A.V. Kadavanich, A.P. Alivisatos, Epitaxial growth of highly luminescent CdSe/CdS core/shell nanocrystals with photostability and electronic accessibility, J. Am. Chem. Soc. 119 (1997) 7019–7029.

[24] S. Yadav, A. Singh, L. Thulasidharan, S. Sapra, Surface decides the photoluminescence of Colloidal CdSe nanoplatelets based core/shell heterostructures, J. Phys. Chem. C. 122 (2018) 820–829.

[25] D.S. He, Z.Y. Li, J. Yuan, Kinematic HAADF-STEM image simulation of small nanoparticles, Micron 74 (2015) 47–53.

[26] N. Fernandez-Delgado, M. Herrera, J. Pizarro, P. Galindo, S.I. Molina, HAADF-STEM for the analysis of core-shell Quantum Dots, J. Mater. Sci. (2018).

[27] R.D. Rajapaksha, M.I. Ranasinghe, The shell thickness and surface passivation dependence of fluorescence decay kinetics in CdSe/ZnS core-shell and CdSe core colloidal quantum dots, J. Lumin. 192 (2017) 860–866.

[28] M. Isarov, N. Grumbach, G.I. Maikov, J. Tilchin, Y. Jang, A. Sashchiuk, E. Lifshitz, The effect of low temperature coating and annealing on structural and optical properties of CdSe/CdS core/shell QDs, Lith. J. Phys. 55 (2015) 297–304.